Vol. 17, pp. 103–112 (2020)
doi: 10.2142/biophysico.BSJ-2020015

Biophysics and Physicobiology
https://www.jstage.jst.go.jp/browse/biophysico/

Regular Article

Spectroscopic and structural characteristics of a dual-light sensor protein, PYP-phytochrome related protein

Jia-Siang Sum[1], Yoichi Yamazaki[1], Keito Yoshida[1], Kento Yonezawa[2], Yugo Hayashi[1], Mikio Kataoka[1] and Hironari Kamikubo[1,2]

[1] *Division of Materials Science, Graduate School of Science and Technology, Nara Institute of Science and Technology, Ikoma, Nara 630-0192, Japan*
[2] *Institute of Materials Structure Science, High Energy Accelerator Research Organization (KEK), Tsukuba, Ibaraki 305-0801, Japan*

Received July 30, 2020; accepted August 26, 2020; Released online in J-STAGE as advance publication September 1, 2020

PYP-phytochrome related (Ppr) protein contains the two light sensor domains, photoactive yellow protein (PYP) and bacteriophytochrome (Bph), which mainly absorb blue and red light by the chromophores of *p*-coumaric acid (*p*CA) and biliverdin (BV), respectively. As a result, Ppr has the ability to photoactivate both domains together or separately. We investigated the photoreaction of each photosensor domain under different light irradiation conditions and clarified the inter-dependency between these domains. Within the first 10 s of blue light illumination, Ppr (Holo-Holo-Ppr) accompanied by both *p*CA and BV demonstrated spectrum changes reflecting PYP_L accumulation, which can also be observed in Ppr containing only *p*CA (Holo-Apo-Ppr), and a fragment of Ppr lacking the C-terminal Bph domain. Although Holo-Apo-Ppr showed PYP_L as a major photoproduct under blue light, as seen in the Bph-truncated Ppr, the equilibrium in the Holo-Holo-Ppr was shifted from PYP_L to PYP_M as the reaction progresses under blue light. Concomitantly, the spectrum of Bph exhibited subtle but distinguishable alteration. Together with the fact, it can be proposed that Bph with BV influences the photoreaction of PYP in Ppr, and vice versa. SAXS measurements revealed substantial tertiary structure changes in Holo-Holo-Ppr under continuous blue light irradiation within the first 5 min time domain. Interestingly, the changes in tertiary structure were partially suppressed by photoactivation of the Bph domain. These observations indicate that the photoreactions of the PYP and Bph domains are coupled with each other, and that the interplay realizes the structural switch, which might be involved in downstream signal transduction.

Key words: bacteriophytochrome, photoactive yellow protein, photoreactions, small-angle x-ray scattering

Corresponding author: Hironari Kamikubo, Division of Materials Science, Graduate School of Science and Technology, Nara Institute of Science and Technology, 8916-5 Takayama-cho, Ikoma, Nara 630-0192, Japan.
e-mail: kamikubo@ms.naist.jp

Introduction

Living organisms have long utilized various light-sensing proteins as a means of survival. Bacteriophytochromes (Bph) are a family of light-sensing proteins that aid in locating food sources or avoiding harm [1–3]. Bph generally contains PAS, GAF, and PHY domains. Biliverdin

◀ ***Significance*** ▶

This study analyzed the spectroscopic and structural characteristics of the Ppr protein to understand the photoreaction of each photosensor domain under different light conditions and elucidate the inter-dependency between the two domains. We believe that our study makes a significant contribution to the literature because no structural information for Ppr has been published to date. Our study is the first to show that PYP and Bph interact and exert an influence on their photoreactions. This interaction results in control of the tertiary structure of Ppr, and might also be responsible for downstream signal transduction via the histidine kinase pathway.

(BV) is a chromophore covalently attached through a cysteine residue in the PHY domain [4]. Typically, Bph photoconverts between stable red (P_r) and metastable far-red (P_{fr}) forms [5,6].

PYP-phytochrome related (Ppr) protein, a member of the bacteriophytochrome family, was found in *Rhodospirillum centenum* (also known as *Rhodocista centenaria*). In addition to the PAS-GAF-PHY photosensory core and a histidine kinase (HK) output domain, Ppr has a photoactive yellow protein (PYP) domain at its N-terminal end [7]. Setting Ppr apart from other classical Bph, Ppr can absorb blue and red light with both *p*-coumaric acid (pCA) and BV depending on the absorption bands of the chromophores. It was reported that Ppr is related to expression regulation of the chalcone synthase gene (*chsA*) [7] and cyst development [8]. Ppr demonstrates higher expression of *chsA* under infrared light, while the presence of blue light suppresses *chsA* expression [7]. The HK domain of Ppr is shown to bind to the chemotactic protein CheW [9]. Furthermore, mutagenic studies of *R. centenum* chemotactic proteins demonstrate a strong relationship between chemotactic response and phototactic response [10,11]. These findings suggest that Ppr plays a role in the phototactic response in *R. centenum*.

Despite sharing a similar domain arrangement of PAS-GAF-PHY with other Bph species, Ppr shows substantially different spectrum changes under red light illumination. Red-light illuminated Ppr demonstrates an apparent decrease in the absorption band around 700 nm instead of accumulation of the red-shifted species P_{fr} [12]. Although studies on other Bph proteins, such as *Dr*BphP, reported that Bph can toggle tertiary structure changes between Pr and Pfr states [13,14]; until now, there was no evidence that Ppr underwent any structural change following stimulation by light. PYP is a blue light-sensing protein found in *Halorhodospira halophila* (*Hh*-PYP) [15]. Over the years, the photocycle model of PYP has become increasingly complex as more studies reveal its underlying mechanisms [16–18]. However, the photocycle can be summarized as the conversion of the ground-state PYP and two photointermediates, the red-shifted intermediate PYP_L (λ_{max}, 490 nm) and the blue-shifted intermediate PYP_M (λ_{max}, 350 nm) [19]. Currently, the transducer protein for PYP remains unknown. Studying the multi-domain protein of Ppr containing the PYP domain provides an opportunity to gain insight into the possible changes to PYP when interacting with other proteins.

In order to study the possible interplay between PYP and Bph within Ppr, an approach to individually photoactivate the chromophore one domain at a time was devised. We prepared Ppr proteins in 3 different apo and holo forms: Ppr containing both pCA and BV; Holo-Holo-Ppr (H-H-Ppr), Ppr containing only BV; Apo-Holo-Ppr (A-H-Ppr), and Ppr containing only pCA; Holo-Apo-Ppr (H-A-Ppr). Spectroscopic data for the Ppr variants, which were subjected to different light irradiation conditions using blue and red light to trigger different Ppr domains, were recorded. To date, there is no available structural information for Ppr. As pointed out by Björling [20], spectroscopic measurements have limitations in that they only reveal the chromophore's local environment. Coupled with spectroscopic data, additional structural information on Ppr would provide a better understanding of the signaling mechanisms of Ppr. We carried out small-angle X-ray scattering (SAXS) measurements on Pprs under light irradiation conditions to probe the tertiary structure change of Ppr against ground state Ppr. These experiments provide valuable knowledge on how Ppr undergoes substantial structural changes. While the other variants showed only PYP_L during the photoreactions, H-H-Ppr accumulated a PYP_M-like photoproduct following PYP_L. Ppr containing PYP_M showed significant structural changes that were suppressed by activating Bph. These results suggest that PYP and Bph interact and exert an influence on their photoreactions. The interplay results in control of the tertiary structure of Ppr, which might be responsible for downstream signal transduction.

Materials and Methods

Protein expression and purification

The double plasmid H-A-Ppr expression system was constructed and transformed into *Escherichia coli* BL21(DE3) as previously reported [21]. The *Rhodobacter capsulatus* TAL and pCL genes were in the pACYCDuet1 vector (Merck, Germany), and the Ppr gene of *R. centenum* was in the pET16b vector. The culture was grown in 800 mL of LB medium containing ampicillin (50 μg/mL) and chloramphenicol (10 μg/mL). At an OD_{600} of 0.4–0.7, IPTG was added to a concentration of 1 mM. Induction was carried out at 20°C for 16 h. Cell pellets were resuspended in 50 mM NaH_2PO_4, 40 mM NaCl, 2% glycerol, and 1 mM DTT (pH 7.4), and disrupted with a sonicator (40% duty cycle, 2 min 5 times, VP-30s, TAITEC, Japan) on ice. The suspension was centrifuged at 30,000×g for 1 h at 4°C (Avanti® HP-26xp, Beckman Coulter, USA). The supernatant was subjected to the following purification steps for H-A-Ppr preparation. To reconstitute H-H-Ppr, an excess amount of BV was added into the supernatant. Crude solutions containing Ppr were applied to the Ni Sepharose™ 6 Fast Flow column (GE Healthcare, USA). H-H-Ppr and H-A-Ppr were eluted from the column by adding a buffer containing 500 mM imidazole. The obtained solution was subjected to size exclusion chromatography (HiLoad 16/60 Superdex 200 pg) installed in the AKTA Explorer (GE Healthcare), where a loading buffer containing 25 mM Tris-HCl, 50 mM NaCl, 2% glycerol, 5 mM EDTA, and 1 mM DTT (pH 8.2) was used. The purified histidine-tagged Ppr was treated with Factor Xa (Novagen) to remove the histidine-tag. Purified H-H-

Ppr was dialyzed in a 500 mM hydroxylamine solution containing 25 mM Tris-HCl, 50 mM NaCl, 2% glycerol, and 5 mM EDTA (pH 8.2) to obtain A-H-Ppr. The reaction was continued until the absorbance at 430 nm did not change. Judging from the agreement between the difference spectrum of A-H-Ppr under blue light irradiation condition and that of H-H-Ppr under red light irradiation condition (see below), it was confirmed that the prepared A-H-Ppr did not contain photoactive pCA in PYP. Bleached Ppr was dialyzed in 25 mM Tris-HCl, 50 mM NaCl, 2% glycerol, 5 mM EDTA, and 1 mM DTT (pH 8.2) to remove hydroxylamine.

UV-visible spectroscopy

UV-visible spectra were recorded using a multichannel spectrometer (QE65000, OCEAN Optics, USA) at 20°C. The buffer conditions used were 25 mM Tris-HCl, 50 mM NaCl, 2% glycerol, and 5 mM EDTA (pH 7.0). A-H-Ppr and H-A-Ppr contained 1 mM DTT to stabilize the sample. Samples were irradiated using a blue LED (λ_{max}=470 nm) and/or a red LED (λ_{max}=630 nm). Before the absorption spectrum measurements were carried out, the Ppr sample was pre-irradiated with red light for 30 min and allowed to recover to the dark state for 7 h to ensure that the measured samples were in the appropriate dark-adapted form.

SAXS measurements

SAXS profiles of the H-H-Ppr protein were collected using the beamline BL-10C in the Photon Factory. X-ray diffraction patterns were recorded using a PILATUS3 2M (Dectris, Switzerland) detector at a wavelength of 1.5 Å. The sample-detector distance was set at 931.2 mm. The cell temperature was maintained at 19.5°C. The sample buffer contained 25 mM Tris-HCl, 50 mM NaCl, 2% glycerol, 5 mM DTT, and 5 mM EDTA. The SAXS profiles of H-A-Ppr and A-H-Ppr were collected using NanoViewer (RIGAKU, Japan) installed at the X-ray source (ultraX 18, RIGAKU). The SAXS profiles were recorded using XII-CCD (HAMAMATSU, Japan) at 20°C. The sample buffer contained 25 mM Tris-HCl, 50 mM NaCl, 2% glycerol, 1 mM DTT, and 5 mM EDTA for both A-H-Ppr and H-A-Ppr. The concentrations were 5.6 mg/mL, 3.7 mg/mL and 1.9 mg/mL for A-H-Ppr and 1.3 mg/mL for H-A-Ppr, respectively.

Results and Discussion

Figure 1 shows the dark state absorption spectra of H-H-Ppr (line 1), A-H-Ppr (line 2), and H-A-Ppr (line 3). H-H-Ppr exhibits two broad peaks around 400 nm and 700 nm, as reported previously [22]. It should be noted that the spectrum in the blue light region had a broad spectrum accompanied by a shoulder near 430 nm, reflecting the superposition of the absorption arising from the PYP and Bph domains. While H-A-Ppr with pCA alone exhibited a single peak at λ_{max} of 430 nm, A-H-Ppr containing only BV in Bph showed dual peaks at 390 nm and 700 nm, which reflect the Soret and Q bands, respectively. The spectrum in the blue light region of H-H-Ppr (line 1) can be reconstructed from the linear combination (line 4) of H-A-Ppr and A-H-Ppr. The good agreement suggests that the PYP and Bph domains in the dark state do not affect each other within Ppr.

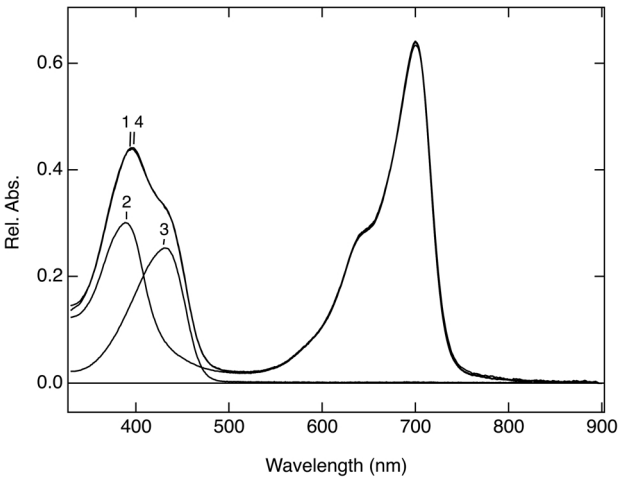

Figure 1 Absorption spectra of Holo-Holo-Ppr (line 1), Apo-Holo-Ppr (line 2,) and Holo-Apo-Ppr (line 3) under dark conditions. The convoluted absorption spectrum of Apo-Holo-Ppr and Holo-Apo-Ppr (line 4) is well superposed on line 1.

Photoreaction of the PYP domain in H-A-Ppr was observed under dark conditions and continuous blue light illumination (λ_{max}=470 nm) (Fig. 2). Blue light irradiation decreased the absorbance around 430 nm (Fig. 2A). The difference spectrum between the light and dark states showed a significant decrease around 430 nm, and a minor increase in absorption around 350 nm and 470 nm (Fig. 2B). The spectral shape closely resembles that of Ppr-PYP (truncated Ppr with only PYP domain) under blue light irradiation [21]. It was reported that Ppr-PYP exhibits equilibrium between PYP_M and PYP_L under continuous blue light irradiation. The positive peak around 470 nm suggests that the equilibrium is shifted from PYP_M to PYP_L [21,23]. From these results, it was found that PYP_L was also stabilized in full-length H-A-Ppr under continuous blue light irradiation.

Figure 3A shows the absorption spectra of A-H-Ppr in the dark and under red light or blue light irradiation. A substantial decrease and a slight increase were found around 700 nm (Q band) and 400 nm (Soret band), respectively. Although red light illumination results in a more significant absorbance decrease around 700 nm than blue light illumination, the scaled difference spectra showed good coincidence (Fig. 3C, lines 1 and 2), indicating that the blue and red lights produced the same photoproduct. Under continuous red light irradiation, H-H-Ppr showed a similar spectrum change to A-H-Ppr (Fig.

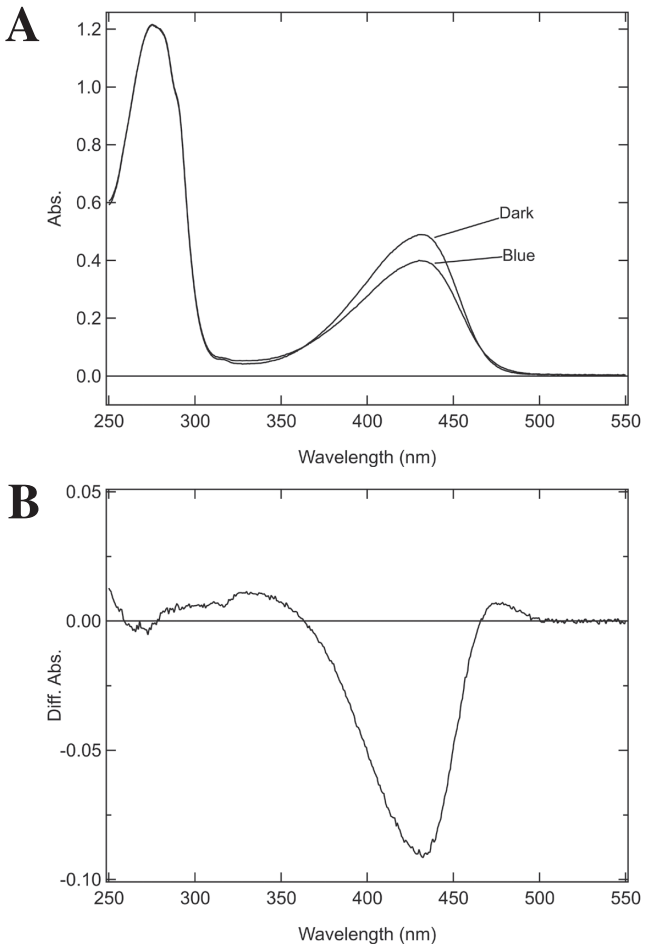

Figure 2 (A) Absorption spectra of H-A-Ppr under dark conditions and blue light irradiation. (B) Blue/dark difference absorption spectrum of H-A-Ppr.

3B). The difference spectrum of H-H-Ppr shown in Figure 3C (line 3) was in good agreement with A-H-Ppr (lines 1 and 2), suggesting that the photoproducts of A-H-Ppr and H-H-Ppr under red light irradiation were identical to each other. From these results, it can be suggested that the dark state of the PYP domain in both H-H-Ppr and A-H-Ppr do not affect the chromophore environment of the Bph domain.

Next, the absorption spectral changes were measured under conditions in which both PYP and Bph were activated. The difference spectrum of H-H-Ppr under simultaneous irradiation of red and blue lights (red+blue) is shown in Figure 4. Assuming that both photo-activated PYP and Bph do not interfere with each other, the observed difference spectrum can be interpreted by the linear combination of H-A-Ppr under blue light (Fig. 2B) and H-H-Ppr under red light (Fig. 3C, line 3). However, the observed difference spectrum of H-H-Ppr could not be reconstructed (Fig. 4). By comparing the calculated difference spectrum and the observed difference spectrum of H-H-Ppr, the spectrum of H-H-Ppr exhibited an

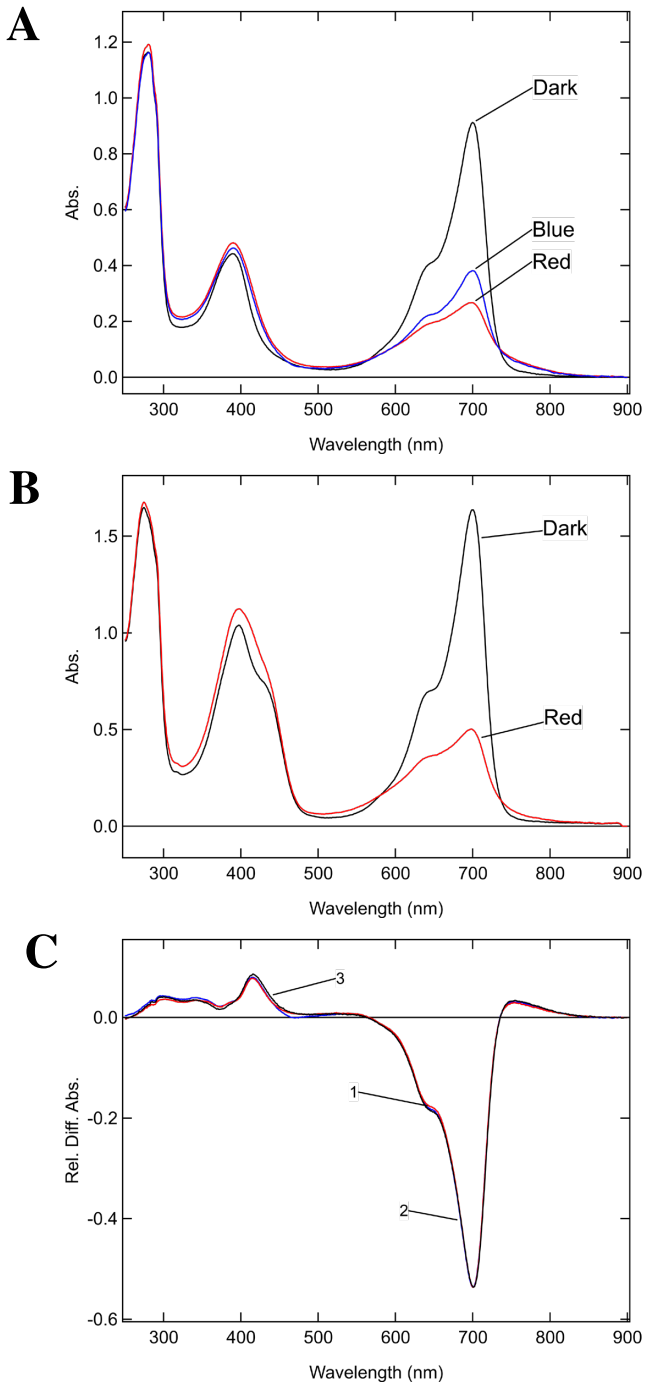

Figure 3 (A) Absorption spectra of A-H-Ppr under dark conditions, red light irradiation, and blue light irradiation. (B) Absorption spectra of H-H-Ppr under the dark and the red light irradiation. (C) Red/dark (line1, red) and blue/dark (line2, blue) difference absorption spectrum of A-H-Ppr (line 1), and red/dark difference absorption spectrum of H-H-Ppr (line 3, black). For the sake of comparison, the difference spectra are normalized to fit the absorbance at 700 nm.

additional increase and decrease in both the blue and red light regions (see the residual plot in Fig. 4). These differences cannot be interpreted by the difference spectra of the individual photo-activated PYP and Bph, suggesting

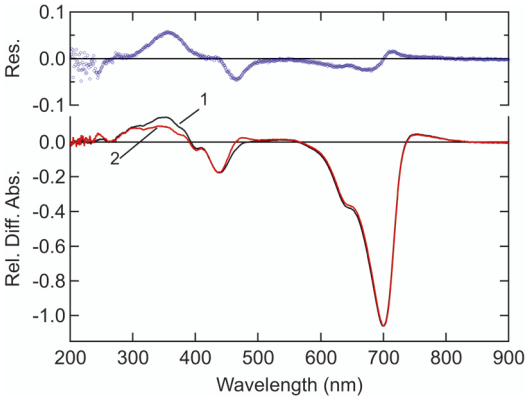

Figure 4 Red+blue/dark difference absorption spectrum of H-H-Ppr are represented by line 1 (black). Calculated difference spectrum of both blue/dark of H-A-Ppr (Fig. 2B) and red/dark of A-H-Ppr (Fig. 3C, line1) are represented by line 2 (red). Residual difference between the two curves are represented by scatter marks above (blue). The calculated difference spectrum was obtained by the summation of scaled blue/dark difference spectra of H-A-Ppr and red/dark difference spectrum of A-H-Ppr. Firstly, the scale factor for the red/dark difference spectrum of A-H-Ppr was obtained to fit the absorbance at 700 nm of the red+blue/dark difference spectrum of H-H-Ppr. The scaled red/dark difference of A-H-Ppr was subtracted from the red +blue/dark difference spectrum of H-H-Ppr, resulting in a double difference spectrum. Finally, the scale factor for the blue/dark difference spectrum of H-A-Ppr was given to fit the absorbance at 430 nm of the double-difference spectrum.

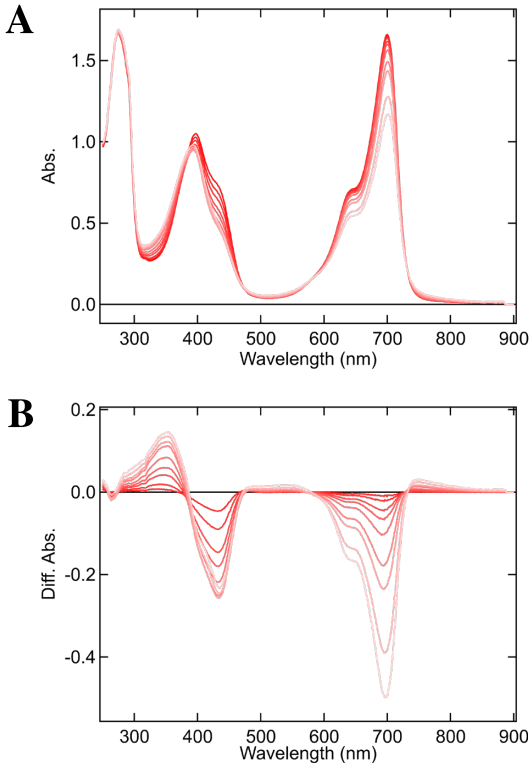

Figure 5 (A) Absorption spectra of H-H-Ppr under blue light irradiation. Each spectrum was irradiated for 0, 10, 20, 40, 60, 100, 200, 300, 800 and 5400 sec from top (deep red) to bottom (light red) at 700 nm. (B) Blue/dark difference absorption spectra of H-H-Ppr. The dark state spectrum was subtracted from the spectrum for each irradiation time in panel A.

that H-H-Ppr in which both chromophores are photo-activated results in different photoproducts compared to those in individually photoactivated PYP and Bph.

To investigate the mutual relationship between photoreactions of PYP and Bph, we measured the spectrum changes of H-H-Ppr from 0 to 90 min under continuous blue light irradiation (Fig. 5), where both PYP and Bph in H-H-Ppr can be activated (Figs. 2 and 3). The gradual increase and decrease in absorbance around 350 nm and 434 nm, respectively (Fig. 5B) reflects photoreaction of both PYP and Bph. The decrease in absorption at around 700 nm results from the photoreaction of Bph. Upon closer inspection, the difference in absorbance spectra under blue light irradiation demonstrated that the absorbance initially decreased at 434 nm, followed by a slight increase, as clearly shown in Figure 6A. The time course of the absorbance changes at 434 nm decreased until 5 min (early phase) and then increased (late phase). The difference spectra between 5 min and 0 min (early phase) and between 90 min and 5 min (late phase) are shown in Figure 6B and C, respectively. The difference spectra in the late phase was similar to those under red light irradiation (Fig. 3C), indicating that the major photoproduct comes from Bph in this time domain. On the other hand, the change in the blue region was relatively larger than in the red region in the early phase, reflecting the photoreaction of PYP. From these results, it can be concluded that PYP and Bph have different rates of photoreactions under blue light. PYP reaches a photo-steady state followed by Bph, which is partly due to the different absorption coefficiency between PYP and Bph at the λ_{max} of the blue LED (470 nm). It should be noted that about 50–60 % of PYP remains to be in the dark state even under the photo-steady state. In addition, careful comparison led us to notice a difference in the λ_{min} around 700 nm. The negative peak was located at 695 nm in the early phase and moved toward 700 nm in the late phase, where the latter value was close to A-H-Ppr and H-H-Ppr, in which only Bph is photo-activated (Fig. 3C). This suggests that the chromophore environment of the Bph domain is perturbed within the early phase of blue light irradiation.

The difference spectra every 5 s from 0 s to 60 s under blue light illumination are shown in Figure 7A. In this time domain, major photoproducts arose from PYP as compared to Bph, although no clear isosbestic point could be found in the spectra. This indicates that there are multiple PYP photoproducts. In order to compare the photoproducts over the reaction time, two difference spectra (10 s–5 s and 30 s–25 s) around 400 nm are representatively shown in Figure 7B and 7C, respectively. The difference spectrum in the initial 10 s (Fig. 7B) closely resembles that of H-A-Ppr under continuous blue light irradiation (Fig. 2B and Supplementary Fig. S1). The positive peak around 470 nm

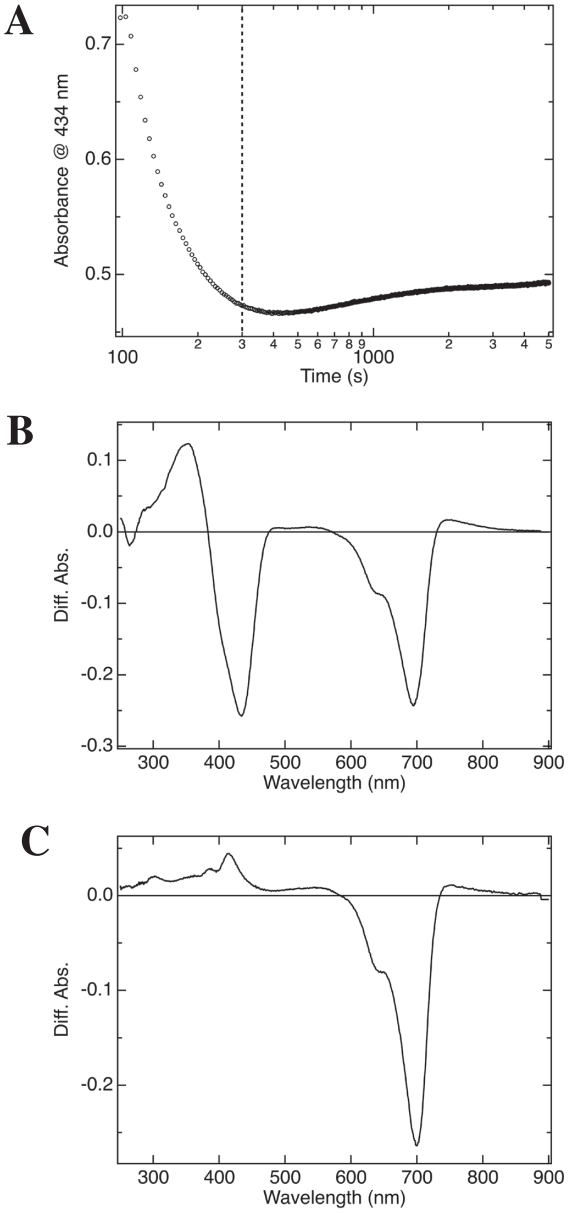

Figure 6 (A) Time-dependent absorbance changes of H-H-Ppr at 434 nm. The reaction curve exhibited different behavior before and after 5 min. The time axis is represented in the logarithmic scale to resolve the early and the late phase time domains. Difference absorption spectra of H-H-Ppr between 5 min and 0 min and between 90 min and 5 min under blue light irradiation are shown in (B) and (C), respectively.

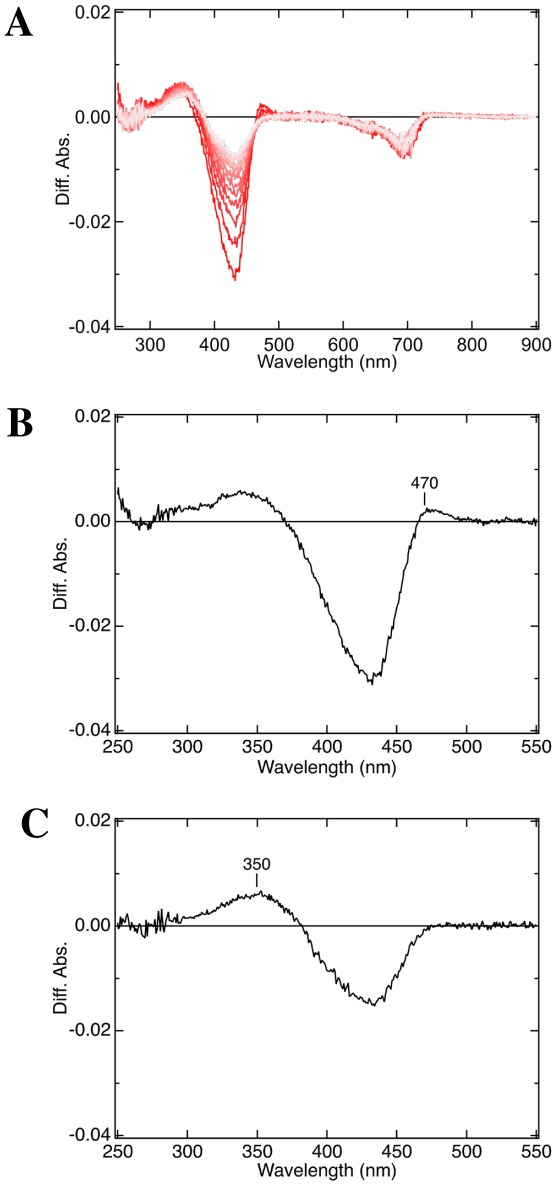

Figure 7 (A) Time-resolved difference spectra of H-H-Ppr at a difference interval of every 5 s under blue-light irradiation (5 s, deep red – 60 s, light red). Difference absorption spectra of PYP between 5 s and 10 s (B) and between 25 s and 30 s (C) are representatively shown.

diminishes after 30 s, and the ratio of the absorbance at 350 nm to 434 nm increased over time (Fig. 7C). These characteristics can also be seen during the formation of PYP_M in *Hh*-PYP [19], indicating that H-H-Ppr induces a subsequent reaction from PYP_L to PYP_M due to holo-Bph, as it cannot be observed in H-A-Ppr.

Because a smaller amount of the photoproduct from Bph accumulated within 30 s in the early phase, the absorption changes can be interpreted as the photoproducts from PYP. However, even in the early phase of the reaction in the 30 s–300 s time domain, the absorption changes reflecting the photoreaction of Bph cannot be neglected, as predicted from the more substantial decrease in absorbance around 700 nm (Fig. 6B). In order to remove the contribution of the Soret band of Bph, the difference spectrum of H-H-Ppr under continuous red-light illumination (Fig. 3C, line 3) was subtracted from those in Figure 5B by multiplying a factor to fit the absorbance at 700 nm, as is explained in Supplementary Figure S2. The relative amplitudes of the absorbance changes at 700 nm in Figure 5B are summarized in Figure 8B, and reflect the increase of the photoproduct of Bph in H-H-Ppr under blue light

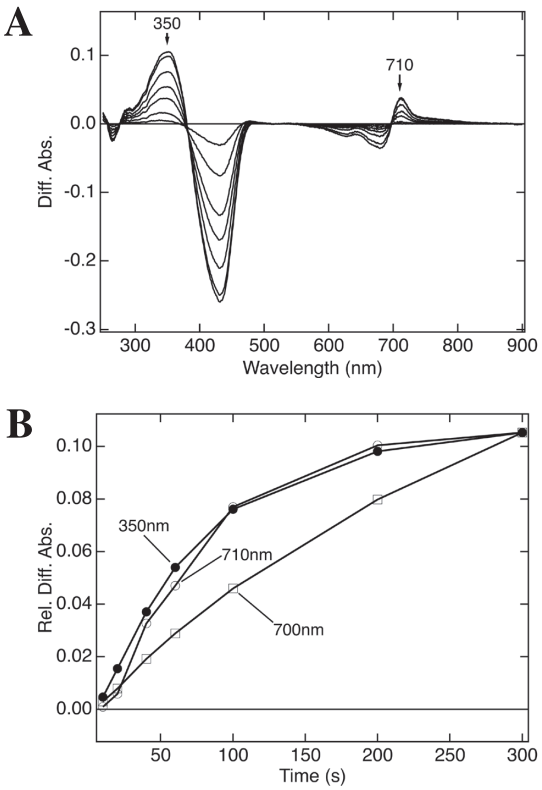

Figure 8 (A) Double difference absorption spectra of H-H-Ppr under blue light irradiation sampled at different times. The black arrows indicate 350 nm and 710 nm. (B) The double difference absorbance at 350 nm and 710 nm in Figure 8A, and the difference absorbance at 700 nm in Figure 5B are shown, and the plots are scaled to fit the values at 300 s.

illumination. The resultant double-difference spectra are shown in Figure 8A. We noticed a residual difference absorption around 700 nm, indicating that the chromophore environment in Bph under blue light differs from that under red light. The double difference spectra in the blue light region agreed with that observed between 30 s and 25 s (Fig. 7C), suggesting that the major photoproduct of PYP after 30 s can be considered as the PYP_M-like state, and the amount of the PYP_M-like state increases with reaction time. Figure 8B shows that the absorbance changes at 350 nm and 710 nm in the double difference are well superposed to each other, but not to that at 700 nm in the difference spectra (Fig. 5B). This indicates that the spectrum change of Bph is coupled with the photoreaction of PYP, but not the reaction of Bph. Based on the facts that the absorption at 350 nm reflects the formation of the PYP_M-like state and the absorption at 710 nm to environmental changes around the Bph chromophore, it can be suggested that the formation of the PYP_M-like state is related to the environmental change in Bph rather than the photoreaction of Bph.

The UV-Vis spectroscopic measurements revealed that PYP in H-H-Ppr showed PYP_M-like photoproducts, but not in H-A-Ppr and the PYP domain alone. Additionally, the

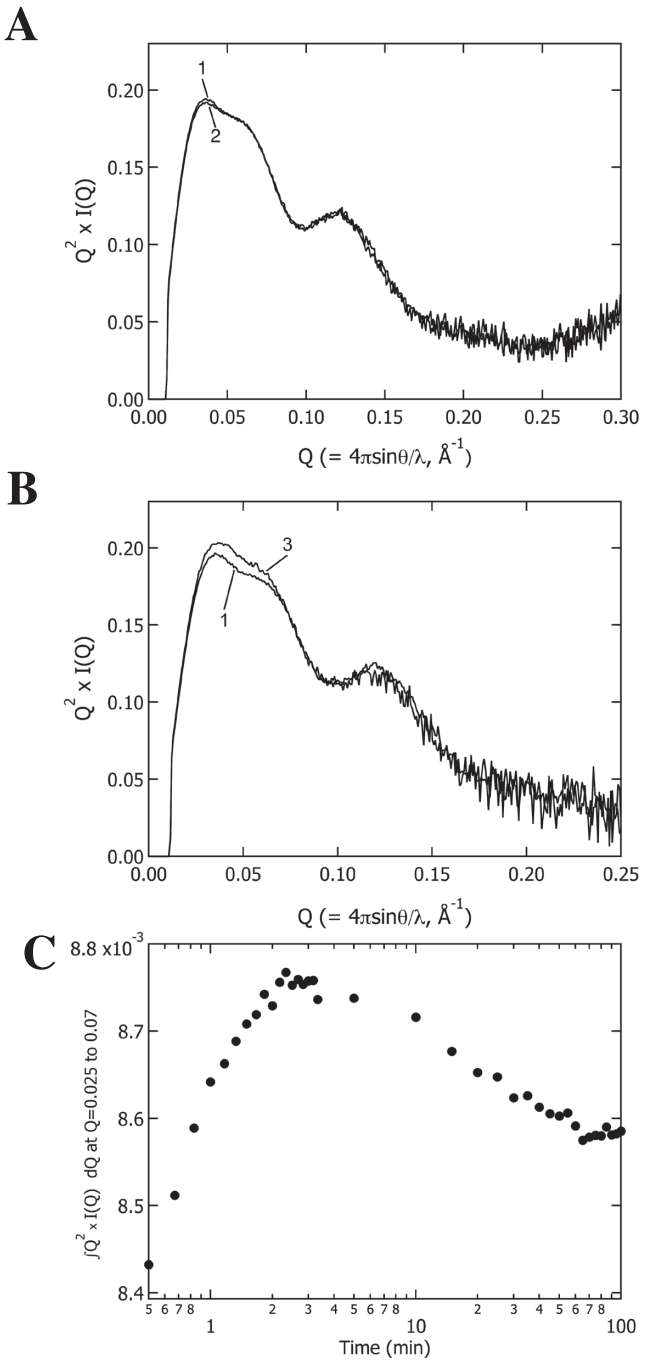

Figure 9 (A) Kratky plots of H-H-Ppr under dark conditions (line 1) and red light irradiation (line 2). (B) Kratky plots of H-H-Ppr under dark conditions (line 1) and 90 s blue light irradiation (line 3). (C) Time course of the dark/blue integrated intensity of the Kratky plots from Q=0.025 to 0.07.

formation of PYP_M-like photoproducts influenced the chromophore environment of Bph. From these results, it can be proposed that H-H-Ppr mediates the mutual relationship between the PYP and Bph domains during the photoreaction, which would be mediated by tertiary structural changes. To investigate changes in the tertiary structure of Ppr during the photoreaction, we carried out

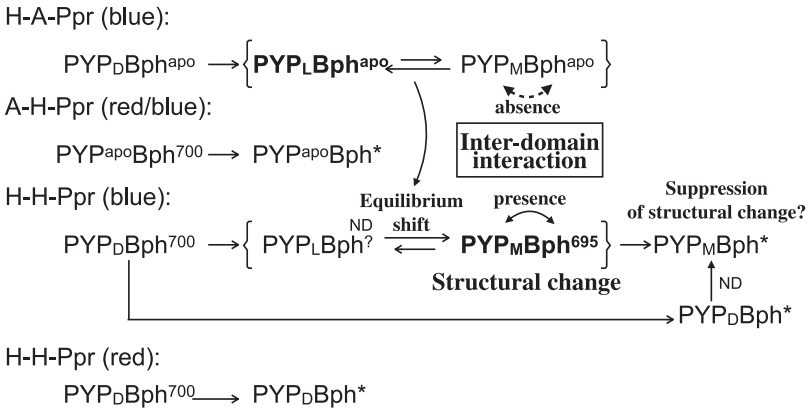

Figure 10 Schematic reactions of H-A-Ppr, A-H-Ppr, and H-H-Ppr, reveled by the current studies. (ND: not detected)

SAXS measurements. The dark state and red light-irradiated H-H-Ppr profiles were almost identical (Fig. 9A), although a slight decrease was found at the peak of 0.04 $Å^{-1}$. The red light triggered the photoreaction in Bph only, indicating that the photoproduct of Bph alone cannot undergo significant tertiary structural changes. The SAXS profiles of A-H-Ppr under red and blue illumination also showed little structural change (Supplementary Fig. S3A).

For H-H-Ppr, the Kratky plots in Figure 9B indicates apparent changes around Q=0.05 $Å^{-1}$ upon blue light irradiation, as cannot be seen in H-A-Ppr (Supplementary Fig. S3B). Figure 9C shows the time dependence of the integrated intensity between 0.025 $Å^{-1}$ and 0.07 $Å^{-1}$. The intensity increased up to 5 min and then decreased, indicating that most structural changes occurred in 5 min. Remembering the photoreaction of H-H-Ppr under blue light illumination (Fig. 6), the absorbance change also showed a similar behavior. This suggests that the structural change is related to the formation of the PYP_M-like photoproduct accumulated during the early phase of the photoreaction. Furthermore, the integrated intensity gradually decreased in the late phase of the photoreaction. Only Bph undergoes photoreaction in this time domain, while PYP has already reached its photo-steady state, as seen in Figure 6C. This suggests that the formation of the PYP_M-like photoproduct promotes the tertiary structural change, while the photoactivation of Bph suppresses the tertiary structure change triggered by the PYP_M-like photoproduct.

We successfully discovered the condition in which Ppr undergoes a tertiary structure change during photoreaction. It was found that the tertiary structural change of Ppr is responsible for photoreaction of PYP in H-H-Ppr. The photoproducts and their structural states are summarized in Figure 10. The difference spectra of H-H-Ppr and A-H-Ppr upon red light illumination are very close to each other, indicating that the same photoproduct of Bph (Bph*) is accumulated in these Pprs regardless of pCA in PYP [H-H-Ppr (red) and A-H-Ppr (red/blue) in Fig. 10]. On the other hand, the photoproduct PYP is highly influenced by the presence of BV in Bph. While H-A-Ppr mainly gave the PYP_L-like photoproduct under blue light illumination [A-H-Ppr (blue) in Fig. 10], H-H-Ppr containing both the chromophores of pCA and BV clearly showed the subsequent equilibrium shift from PYP_L to PYP_M [H-H-Ppr (blue) in Fig. 10]. This suggests that Bph accompanied by BV influences the chromophore environment of PYP during photoreaction. This was also confirmed by the slight shift of the Q band of Bph in H-H-Ppr during PYP_M-like photoproduct formation [H-H-Ppr (blue) in Fig. 10]. Concerning the structural aspects, there are few structural changes in both H-H-Ppr and A-H-Ppr under red light illumination, triggering the photoreaction of Bph. Although H-A-Ppr did not show tertiary structural changes, the SAXS measurements of H-H-Ppr under blue light illumination revealed noticeable structural changes. As mentioned above, H-A-Ppr and H-H-Ppr result in different major photoproducts under blue light illumination, which are PYP_L and PYP_M, respectively.

Conclusions

From these results, we propose that PYP_M of H-H-Ppr is an active photoproduct responsible for tertiary structural changes which can interact with holo-Bph to stabilize PYP_M (Fig. 10). Previous studies on *Hh*-PYP revealed that PYP_M is a putative active intermediate that takes a partially unfolded structure in the N-terminal region [24]. Assuming PYP_M of H-H-Ppr also undergoes similar structural changes, it can be expected that the structural change can affect interaction with the neighboring Bph domain. The slight shift of the UV-Vis spectrum of Bph depending on PYP_M accumulation would reflect alteration of the inter-domain interaction triggered by the structural change in PYP. For the late phase of the reaction initiated by blue light irradiation, the UV-Vis measurements indicate that the photoreaction involves only the formation of the Bph photoproduct. Within this time domain, the SAXS

measurements revealed that the structural difference between the light state and the dark state was reduced. We speculate that the tertiary structure change induced by PYP_M would partially or fully recover to that of the original dark state due to photoactivation of Bph. If the tertiary structure is closely related to histidine kinase activity, the histidine kinase activity changes triggered by PYP_M would be retrieved when the photoproduct of Bph is accumulated by intense blue or red light illumination. In conclusion, Ppr can modulate histidine kinase activity, which is increased (or decreased) by blue light and decreased (or increased) by red light. Further studies on the relationship between structural changes and histidine kinase activity will provide clues to understanding the photoregulation of Ppr responsible for downstream signaling.

Acknowledgements

This work is partly supported by Grants-in-Aid from JSPS for Scientific Research (Category S, No. JP17H06165 (H.K.); Innovative Areas, No. JP25102003 (H.K.)). The SAXS experiments were performed under the approval of the Photon Factory Program Advisory Committee (Proposal No. 2016G077 and No. 2018G119).

Conflicts of Interest

All authors declare that they have no conflict of interest.

Author Contributions

JS, YY, MK, and HK conceived the project and designed the research. JS, YY, KY, and YH carried out the research. KY performed small-angle x-ray scattering analysis. JS, YY and HK wrote the paper. All the authors approved the final version of the manuscript.

References

[1] Davis, S. J., Vener, A. V. & Vierstra, R. D. Bacteriophytochromes: phytochrome-like photoreceptors from nonphotosynthetic eubacteria. *Science* **286**, 2517–2520 (1999). DOI: 10.1126/science.286.5449.2517

[2] Giraud, E. & Verméglio, A. Bacteriophytochromes in anoxygenic photosynthetic bacteria. *Photosynth. Res.* **97**, 141–153 (2008). DOI: 10.1007/s11120-008-9323-0

[3] Auldridge, M. E. & Forest, K. T. Bacterial phytochromes: more than meets the light. *Crit. Rev. Biochem. Mol. Biol.* **46**, 67–88 (2011). DOI: 10.3109/10409238.2010.546389

[4] Montgomery, B. L. & Lagarias, J. C. Phytochrome ancestry: sensors of bilins and light. *Trends Plant Sci.* **7**, 357–366 (2002). DOI: 10.1016/S1360-1385(02)02304-X

[5] Giraud, E., Fardoux, J., Fourrier, N., Hannibal, L., Genty, B., Bouyer, P., *et al.* Bacteriophytochrome controls photosystem synthesis in anoxygenic bacteria. *Nature* **417**, 202–205 (2002). DOI: 10.1038/417202a

[6] Rottwinkel, G., Oberpichler, I. & Lamparter, T. Bathy phytochromes in rhizobial soil bacteria. *J. Bacteriol.* **192**, 5124–5133 (2010). DOI: 10.1128/JB.00672-10

[7] Jiang, Z.-Y., Swem, L. R., Rushing, B. G., Devanathan, S., Tollin, G. & Bauer, C. E. Bacterial photoreceptor with similarity to photoactive yellow protein and plant phytochromes. *Science* **285**, 406–409 (1999). DOI: 10.1126/science.285.5426.406

[8] Berleman, J. E., Hasselbring, B. M. & Bauer, C. E. Hypercyst mutants in Rhodospirillum centenum identify regulatory loci involved in cyst cell differentiation. *J. Bacteriol.* **186**, 5834–5841 (2004). DOI: 10.1128/JB.186.17.5834-5841.2004

[9] Kreutel, S., Kuhn, A. & Kiefer, D. The photosensor protein Ppr of Rhodocista centenaria is linked to the chemotaxis signaling pathway. *BMC Microbiol.* **10**, 281 (2010). DOI: 10.1186/1471-2180-10-281

[10] Jiang, Z.-Y., Gest, H. & Bauer, C. E. Chemosensory and photosensory perception in purple photosynthetic bacteria utilize common signal transduction components. *J. Bacteriol.* **179**, 5720–5727 (1997). DOI: 10.1128/jb.179.18.5720-5727.1997

[11] Jiang, Z.-Y., Rushing, B. G., Bai, Y., Gest, H. & Bauer, C. E. Isolation of RhodospirillumcentenumMutants Defective in Phototactic Colony Motility by Transposon Mutagenesis. *J. Bacteriol.* **180**, 1248–1255 (1998). DOI: 10.1128/JB.180.5.1248-1255.1998

[12] Kyndt, J. A., Fitch, J. C., Meyer, T. E. & Cusanovich, M. A. The photoactivated PYP domain of Rhodospirillum centenum Ppr accelerates the recovery of the bacteriophytochrome domain after white light illumination. *Biochemistry* **46**, 8256–8262 (2007). DOI: 10.1021/bi700616j

[13] Takala, H., Björling, A., Berntsson, O., Lehtivuori, H., Niebling, S., Hoernke, M., *et al.* Signal amplification and transduction in phytochrome photosensors. *Nature* **509**, 245–248 (2014). DOI: 10.1038/nature13310

[14] Burgie, E. S., Zhang, J. & Vierstra, R. D. Crystal structure of Deinococcus phytochrome in the photoactivated state reveals a cascade of structural rearrangements during photoconversion. *Structure* **24**, 448–457 (2016). DOI: 10.1016/j.str.2016.01.001

[15] Meyer, T. E. Isolation and characterization of soluble cytochromes, ferredoxins, and other chromophoric proteins from the halophilic phototrophic bacterium Ectothiorhodospira halophila. *Biochim. Biophys. Acta Bioenerg* **806**, 175–183 (1985). DOI: 10.1016/0005-2728(85)90094-5

[16] Meyer, T. E., Yakali, E., Cusanovich, M. A. & Tollin, G. Properties of a water-soluble, yellow protein isolated from a halophilic phototrophic bacterium that has photochemical activity analogous to sensory rhodopsin. *Biochemistry* **26**, 418–423 (1987). DOI: 10.1021/bi00376a012

[17] Hoff, W. D., Van Stokkum, I. H., Van Ramesdonk, H. J., Van Brederode, M. E., Brouwer, A. M., Fitch, J. C., *et al.* Measurement and global analysis of the absorbance changes in the photocycle of the photoactive yellow protein from Ectothiorhodospira halophila. *Biophys. J.* **67**, 1691–1705 (1994). DOI: 10.1016/S0006-3495(94)80643-5

[18] Imamoto, Y., Kataoka, M. & Tokunaga, F. Photoreaction cycle of photoactive yellow protein from Ectothiorhodospira halophila studied by low-temperature spectroscopy. *Biochemistry* **35**, 14047–14053 (1996). DOI: 10.1021/bi961342d

[19] Imamoto, Y., Harigai, M. & Kataoka, M. Direct observation of the pH-dependent equilibrium between L-like and M intermediates of photoactive yellow protein. *FEBS Lett.* **577**, 75–80 (2004). DOI: 10.1016/j.febslet.2004.09.065

[20] Björling, A., Berntsson, O., Takala, H., Gallagher, K. D., Patel, H., Gustavsson, E., *et al.* Ubiquitous structural

signaling in bacterial phytochromes. *J. Phys. Chem. Lett.* **6**, 3379–3383 (2015). DOI: 10.1021/acs.jpclett.5b01629

[21] Kamikubo, H., Koyama, T., Hayashi, M., Shirai, K., Yamazaki, Y., Imamoto, Y., *et al.* The Photoreaction of the Photoactive Yellow Protein Domain in the Light Sensor Histidine Kinase Ppr is Influenced by the C-terminal Domains. *Photochem. Photobiol.* **84**, 895–902 (2008). DOI: 10.1111/j.1751-1097.2008.00322.x

[22] Kyndt, J. A., Fitch, J. C., Seibeck, S., Borucki, B., Heyn, M. P., Meyer, T. E., *et al.* Regulation of the Ppr histidine kinase by light-induced interactions between its photoactive yellow protein and bacteriophytochrome domains. *Biochemistry* **49**, 1744–1754 (2010). DOI: 10.1021/bi901591m

[23] Imamoto, Y., Kataoka, M. & Liu, R. S. H. Mechanistic Pathways for the Photoisomerization Reaction of the Anchored, Tethered Chromophore of the Photoactive Yellow Protein and its Mutants. *Photochem. Photobiol.* **76**, 584–589 (2002). DOI: 10.1562/0031-8655(2002)0760584MPFTPR2.0.CO2

[24] Imamoto, Y. & Kataoka, M. Structure and photoreaction of photoactive yellow protein, a structural prototype of the PAS domain superfamily. *Photochem. Photobiol.* **83**, 40–49 (2007). DOI: 10.1562/2006-02-28-IR-827

(*Edited by Haruki Nakamura*)